Non destructive transient thermal evaluation of delaminations inside a laminate: a thermal processing technique of thermal images

by D. MAILLET, S. DIDIERJEAN, A.S. HOULBERT
and A. DEGIOVANNI (*)

(*) Laboratoire d'Energétique et de Mécanique Théorique et Appliquée, URA CNRS 875 ENSEM, 2 avenue de la Forêt de Haye, F-54500 Vandoeuvre Les Nancy, France.

Abstract

Delaminations in laminate composite slabs can be detected and measured using a heat pulse excitation on one side and temperature measurement through infrared thermography on either side of the slab. The delamination is characterized in terms of its depth, thermal contact resistance (thickness) and transverse extent. An identification method of the first two defect parameters is developed and experimentally validated. It uses, as input, the Laplace transforms of a local contrast thermogram and, as output, thickness and depth profiles of the possible delamination.

Nomenclature

a	diffusivity	α	square root of the reduced Laplace variable $p^*(= e^2 \, p/a)$
c	specific heat	λ	conductivity
e	thickness	ρ	mass density
e_1, e_2	thickness of the two layers on each side of the defect	θ	Laplace transform of temperature
M	experimental Laplace transform of the contrast ΔT^*		
p	Laplace variable	**Subscripts**	
Q	energy by unit area	$*$	reduced quantity (dimensionless)
r	radial direction	d	delamination
R_C	contact resistance	r	radial direction
T	temperature ($=0$ at $t = 0$)	$1,2$	relative to each layer 1 or 2
t	time	f	front side
x^*	reduced depth of the defect ($=e_1/e$)	r	rear side
z	axial direction	0	relative to sane slab

1. Introduction

Thermal non destructive evaluation (NDE) of composite materials is rapidly developing for a few years [1 to 11]. It is mainly due to the technical progresses in the fields of transient infrared thermography and of rapid data acquisition systems for a later processing on a computer. In these techniques, the part to be checked can be stimulated through photothermal excitation, while the temperature field on part of its surface is monitored using infrared radiometry. The presence of a possible defect affects the internal heat diffusion process and therefore modifies the measured surface temperature field, allowing therefore the detection of a defect.

This work is focused on delamination defects, that is air gaps between two plies of the laminate. Let use note that the complete NDE process of a part requires first the detection of a possible anomaly at some location, second the identification of its nature (discrimination) and third the estimation (measurement) of its parameters (size, depth...). The method presented here concerns the third point, even if point one constitutes a direct output.

2. Thermal non destructive evaluation method

2.1. Defect characterization

A delamination located in a composite slab of infinite radial (r) extent is outlined in *figure 1*. This slab can be a carbon fiber reinforced polymer where the number of plies is big enough to allow the use of homogenized equivalent axial (z) thermal properties (diffusivity a and conductivity λ) and where the periodical shift of the in-plane fiber orientation makes the material isotropic in this plane with radial (or transverse) properties a_r and λ_r. If this delamination (d) is occupied by an air layer of infinite radial extent of conductivity λ_d and of thickness e_d (a few micrometers) small compared to the total slab thickness e (= $e_1 + e_2$), it can be characterized by a contact resistance R_c (=e_d / λ_d) surrounded by two external layers (*1* and *2*) of sane material. Its depth e_1, beneath the heated front side, is its second parameter.

2.2. Thermal contrast

The previous characterization is valid for a one-dimensional (1D) transient heat transfer created for example by a homogeneous heat pulse on the slab front side, with an absorbed energy by unit area Q.

In that case, if the initial temperature of the slab is uniform (=0) and if heat losses are neglected, the heat equation can be solved for each layer. The thermograms, which are the temperature T versus time t curves, can be constructed, for the front side (z =0) or rear side ($z = e$) of the slab.

If temperature is divided by its asymptotic value ($Q/\rho c e$), in order to get rid of the unknown absorbed energy density Q, a normalized T^* thermogram can be obtained for a defective slab ($R_c \neq 0$) and a similar T_0^* one for a sane slab ($R_c = 0$). These reduced thermograms are plotted versus reduced time t^* (Fourier number = at/e^2) in *figures 2a* (front side) and *2b* (rear side). In the same figures, the difference of the two curves $\Delta T^* (= T^* - T_0^*)$, the contrast thermogram, is also plotted. This bell-shape curve contains the complete information about the delamination and constitutes its signature.

2.3. Identification method

One has shown [8 , 9] that the Laplace transform $\Delta \theta^{**}$ of this contrast ΔT^* has the following expression for front (subscript f) or rear (subscript r) detection :

$$\Delta \theta_f^{**} = \frac{R_c^* \sinh^2 [\alpha(1 - x^*)]}{\sinh(\alpha)\{\sinh(\alpha) + R_c^* \, \alpha \sinh(\alpha x^*) \sinh[\alpha(1 - x^*)]\}} \tag{1}$$

$$\Delta \theta_r^{**} = - \frac{R_c^* \sinh(\alpha x^*) \sinh[\alpha(1 - x^*)]}{\sinh(\alpha)\{\sinh(\alpha) + R_c^* \, \alpha \sinh(\alpha x^*) \sinh[\alpha(1 - x^*)]\}} \tag{2}$$

with :
$$\Delta \theta^{**} = \int_0^\infty \exp(-p^* t^*) \Delta T^* \, dt^* \quad ; \quad R_c^* = \frac{R_c}{e/\lambda} \quad ; \quad x^* = \frac{e_1}{e} \quad ; \quad \alpha = \sqrt{p^*} \tag{3}$$

Equations (1 to 3) show that contrast ΔT^* is a function of time t (or t^*) and of the two parameters R_c^* and x^* of the defect, while its reduced transform $\Delta \theta^{**}$ depends on the same parameters and on the reduced Laplace variable p^*. One very interesting feature of $\Delta \theta^{**}$ is that it can be easily calculated, starting from an experimental contrast curve $\Delta T^* (t^*$ or $t)$ through

213

numerical time integration - see equation (3). Starting from equations (1) and (2), written for two values p_1^* and p_2^* $(= 4\ p_1^*)$ of p^*, one can show [8,9] :

$$R_c^* = \frac{M_1^2\ [1 + \alpha_2 \sinh(\alpha_2)M_2]\ \sinh(\alpha_1)\ \tanh(\alpha_1)}{[1 + M_1\alpha_1 \sinh(\alpha_1)][-M_1 + M_2\ \cosh(\alpha_1) - 1.5\ M_1\ M_2\ \alpha_1 \sinh(\alpha_2)]} \qquad (4)$$

with : $\alpha_i = \sqrt{p_i^*}$ and $M_i = \Delta\theta_r^{**}\ (p_i^*, R_c^*, x^*)$ for $i = 1,2$

using rear-side contrast (exact expression) and :

$$x^* = 1 - \frac{1}{\alpha_1}\ \ln\left[\left(\frac{M_2}{M_1}\right)^{1/2} \cosh(\alpha_1) + \left(\frac{M_2}{M_1} \cosh^2(\alpha_1) - 1\right)^{1/2}\right] \qquad (5)$$

214   using front-side contrast (approximate expression, valid for small R_c^*'s or delaminations close to one of the two faces of the slab) with :

$\alpha_i = \sqrt{p_i^*}$ and $M_i = \Delta\theta_f^{**}\ (p_i^*, R_c^*, x^*)$ for $i = 1,2$

3. Experimental results

3.1. Measurement technique

A test slab (360 x 200 mm, 2 mm thick) made out of T300 Carbon epoxy laminate (14 plies) containing artificial delaminations made of disk-shape Teflon films of various thicknesses, depths and radii (manufactured by the Dassault Company) has been used to validate this NDE technique. Heat pulse excitation was produced by a square assembly of four flash tubes located on the focal lines of four cylindro-parabolic reflectors (MECIR stimulation system). The temperature field on either the front or rear side of the test slab was recorded by a 782 SW AGA infrared scanner and acquisition and data storage was done on a DATAMIN board and software plugged into a 386 PC computer.

In real experimental conditions a sane reference slab is seldom available and the reference $T_0(t)$ thermogram can be measured, during a unique experiment, on locations where the temperature is uniformly hot (rear side) or cold (front side) on the monitored frames.

Normalization is also done on a local basis, each T or T_0 thermogram being divided by its local final value - maximum in rear side and minimum in front side as shown on *figures 2*. The result of these normalizations is a contrast ΔT^* that does not depend on the non-uniformity of both emissivity and absorbed energy Q. Experimental Laplace transforms of the contrast, M_1 and M_2 -see first equation (3) - can be calculated and reduced resistances R_c^* (rear side) or reduced depths x^* can be calculated on a point basis.

3.2. Experimental results

The thermal frames of two flash experiments corresponding to rear - *colour illustration A* - and front side detection - *colour illustration B* - have been processed using the above described technique.

A line BB' passing through the centers of defects B4 to B1 (nominal $R_c = 2.10^{-4}$ m^2.K.W^{-1} ; nominal $x^* = 0.36, 0.5, 0.71$ and 0.86 for front side detection ; radius : 10 mm) has been studied and the identified R_c and x^* profiles are plotted on *figures 3 and 4*.

* The colour plates of this article 32 are located on page X of the colour gathering, at the end of the book

For rear side detection, one can notice that the identified R_C's (corresponding to equivalent air thickness) are about two times higher than the nominal ones (except for defect B2 where there is a 6 factor). These over-resistances may stem from air delaminations between the two 25 μm teflon sheets of the artificial defect (hypothesis confirmed by an ultrasonic image).

For front side detection, the agreement between nominal and identified depths is better, differences staying always lower than 6% (of the slab thickness) even if edge effects can affect the defect B4's identified depth.

In another rear side detection experiment, one of the four flash tubes could not operate properly (no heat pulse production for this tube). Figure 5a shows the absolute contrast profile $\Delta T (= T - T_0)$ for the same line of B defects as before at 2.16 s after the pulse : it is very much affected by radial heat transfer since its base line is tilted with respect to the horizontal.

In figure 5b the locally normalized contrast ΔT^* profile is plotted for the same experiment : the previous tilt in the base line is strongly reduced. The corresponding R_C profile is shown in figure 5c : it is very much consistent with the one obtained from the first experiment - see figure 3 - in spite of the highly non homogeneous front side excitation.

4. Conclusion

215

These results yielded by the thermal NDE technique and by data processing through contrast normalization on a local base followed by Laplace transformation, seem to be very promising. One feature of this quantitative infrared method is that it completely departs from classical thermal image processing techniques and rather constitutes a thermal processing of transient intensity fields. Its main advantages can be quoted :

- an important area can be checked in one experiment, even if heat absorption is not perfectly uniform;
- no surface treatment or painting of the part to be checked is necessary (it is a truly non contact technique by opposition to ultrasonic NDE);
- an integral technique is used that reduces the measurement noise (Laplace transform filtering);
- detection is straightforward and delamination diameters can be estimated using contact resistance profiles;
- production of delamination depth or thickness profiles can be automated and the same is true for the creation of depth or tickness images.

REFERENCES

[1] VAVILOV (V.P.) and TAYLOR (R.). - Research Techniques in NDT, Ed. 5, Academic Press, London, 1982.
[2] BALAGEAS (D.), KRAPEZ (J.C) and CIELO (P.). - Pulsed photothermal modeling of layered materials. J. Appl. Phys., 59, 1986, 348-357.
[3] BOSCHER (D.M.), DEOM (A.A.), GARDETTE (G.) and BALAGEAS (D.). - Thermal NDT of carbon epoxy laminates. Proc. Eurotherm 4, Nancy, June 28-29, 1988, 112-115.
[4] CIELO (P.), MALDAGUE (X.), DEOM (A.A.) and LEWARK (R.). - Thermographic non destructive evaluation of industrial materials and structures. Material Evaluation, 45,1987, 452-466.
[5] LAMINE (A.S.), MAILLET (D.) et DEGIOVANNI (A.). - Modélisation et détection d'un défaut limité dans un matériau composite. Proc. Eurotherm 4, Nancy, June 28-29, 1988, 101-104.
[6] LAMINE (A.S). - Caractérisation de defauts dans les matériaux composites par thermographie infrarouge. Thesis, INPL Nancy, nov. 1988.
[7] HOULBERT (A.S.), LAMINE (A.S) et DEGIOVANNI (A.). - Modélisation d'un défaut limité en vue du contrôle non destructif des multimatériaux isotropes. Int. J. Heat Mass Transfer, 34, 4/5, 1991, 1125-1138.
[8] MAILLET (D.), HOULBERT (A.S.), DIDIERJEAN (S.) and DEGIOVANNI (A.). - Identification of a contact resistance located at any depth inside a laminated composite material using experimental Laplace transforms and thermography. Proc. 4th Annual Inverse Problems in Engineering Seminar, East lansing, Michigan, June 10-11, 1991.
[9] MAILLET (D.). - Apport des méthodes analytiques à l'identification des paramètres et à la conduction inverse en thermique. Thèse d'Etat, INPL Nancy, dec.20, 1991.

[10] VAVILOV (V.P.), DEGIOVANNI (A.), DIDIERJEAN (S.), MAILLET (D.),SENGOULIER (A.A.) and HOULBERT (A.S.) - *Thermal flaw detection and tomography of carbon fiber - reinforced articles.* The Soviet Journal of Non Destructive Testing, 609-619, Plenum Pub. Corp., 1992, translated from Defektoskopiya,*9*, 3-14, sept. 1991.

[11] MAILLET (D.), HOULBERT (A.S), DIDIERJEAN (S.), LAMINE (A.S.) and DEGIOVANNI(A.). - *Non destructive thermal evaluation at LEMTA-Delaminations inside a laminate : the identification problem*, Article ref.58/59-A92-431, to be published in Composites Science and Technology.
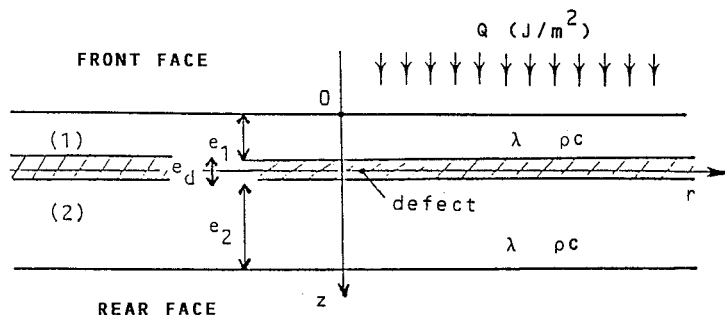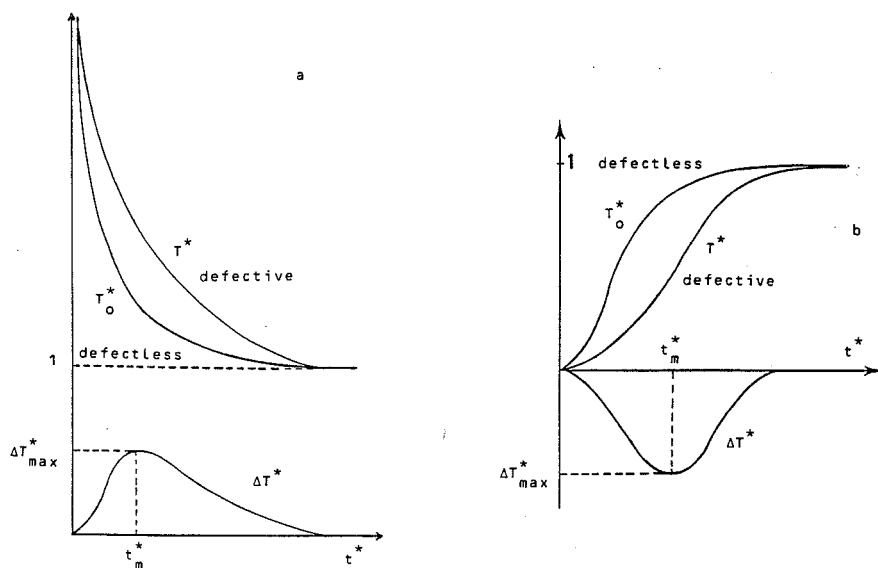
16

Fig. 1. - Geometry of the one-dimension model

Fig. 2. - Thermograms and contrasts
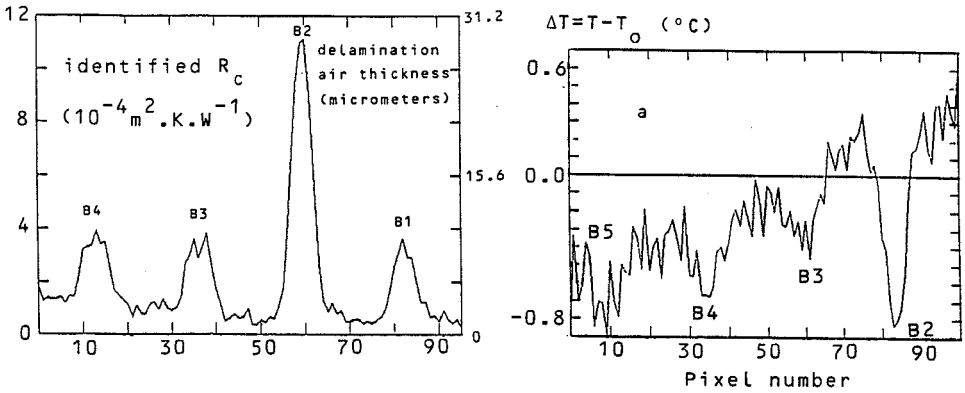
a - front side detection
b - rear side detection

identified R$_c$

(10^{-4}m^2.K.W^{-1})

delamination
air thickness
(micrometers)

B2

B4   B3   B1

Fig. 3.- Identified contact resistance R$_c$ B-B' profile

$\Delta T = T - T_o$ (°C)

a

B5   B4   B3   B2

Pixel number

217

$\Delta T* = T* - T*_o$
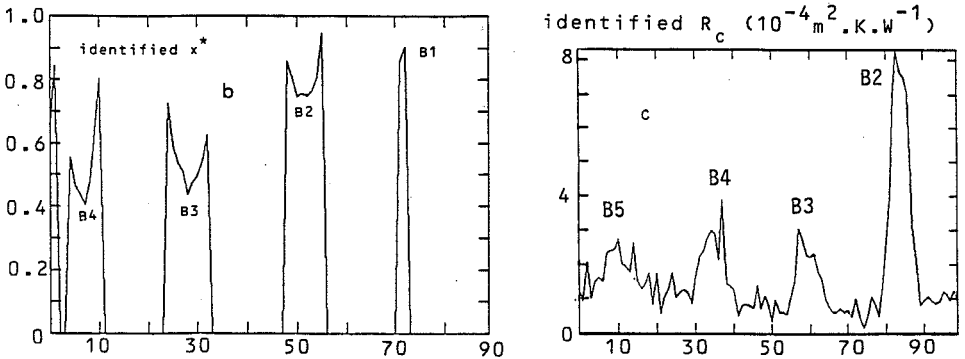
B5   B4   B3   b   B2

Pixel number

identified x*

b

B4   B3   B2   B1

Fig. 4. - Identified reduced depth x* (defect depth beneath front side divided by slab thickness) B-B' profile

identified R$_c$ (10^{-4}m^2.K.W^{-1})

c

B5   B4   B3   B2

Fig. 5. - Rear side experiments with defectuous stimulation B defects

a - absolute contrast ΔT profile (t =2.16 s)
b - contrast $\Delta T*$ profile (t =2.16 s)
c - identified resistance R$_c$ profile